

# Modeling Radio Wave Propagation in Tunnels with a Vectorial Parabolic Equation

Alexei V. Popov, *Member, IEEE*, and Ning Yan Zhu, *Member, IEEE*

**Abstract**—To study radio wave propagation in tunnels, we present a vectorial parabolic equation (PE) taking into account the cross-section shape, wall impedances, slowly varying curvature, and torsion of the tunnel axis. For rectangular cross section, two polarizations are decoupled and two families of adiabatic modes can be found explicitly, giving a generalization of the known results for a uniform tunnel. In the general case, a boundary value problem arises to be solved by using finite-difference/finite-element (FD/FE) techniques. Numerical examples demonstrate the computational efficiency of the proposed method.

**Index Terms**—Adiabatic modes, radio wave propagation in curved tunnels, three-dimensional (3-D) numerical modeling, vectorial parabolic equation (PE).

## I. INTRODUCTION

**V**HF/UHF radio wave propagation in tunnel environments has been a research subject for a long time (see [1]). Recent interests in this subject have been aroused in the wake of the development of mobile communication systems. Two methods are mainly in use: geometrical optics (GO) [2]–[6] and modal analysis [7]–[9].

The GO analysis is complicated at long ranges due to the growing number of contributing rays and breaks down in caustic regions. It must be remembered that multiple caustics occur both in straight tunnels and especially in curved waveguides [10], where propagating modes of the whispering gallery type [11] may be excited. While reasonable numerical results can be obtained by estimating wave amplitudes via the calculated ray density [3], [4], [6], this approach requires excessive computational work and may produce artifacts due to the aforementioned reason. So, apart from extremely high-frequency problems, a full wave solution seems to be preferable. The analogy between a tunnel and a common electromagnetic (EM) waveguide suggests the application of the modal approach. However, this theory is only useful in rare cases of a small number of dominant propagating modes in a uniform waveguide, not to mention the difficulty of determining the eigenfunctions for a real tunnel.

An extension of the modal approach to a more general class of wide (compared with the wavelength) smoothly curved waveguides has been presented in [12]. It has been shown that in the

case of wave packets propagating along the waveguide axis with small Brillouin angles an approximate separation of the longitudinal variable is possible for smoothly nonuniform lossy waveguides of arbitrary cross section. The asymptotic analysis generates a discrete set of low-order vectorial “adiabatic” modes depending on the local value of the waveguide axis curvature. Like in rigorous modal theory, they can be superimposed to represent an arbitrary paraxial wave packet. In practice, only such paraxial modes survive at large distances, because the waveguide wall absorption usually has a minimum at grazing angles. This derivation is laid out in Section II with a generalization to include the case of an arbitrary three-dimensional (3-D) curved axis when the torsion effects may be of importance.

Although adiabatic mode theory enables one to study radio wave propagation in realistic tunnels, it is not always convenient for practical applications because of the remaining computational difficulties (solving the eigenvalue problem for complicated tunnel profiles and numerical summation of the eigenfunctions in a multimode situation). In this respect, a straightforward marching method, like the well-known parabolic wave equation [13]–[15] would better fit the engineers’ needs. The parabolic equation (PE) seems to be an adequate mathematical model of wave propagation in tunnels due to selective wall absorption filtering out higher Brillouin angles and forming a paraxial wave packet, even if the waveguide axis is not a straight line but a smooth curve. A similar situation of scalar guided waves in smoothly nonuniform media has been studied in [16] with the parabolic equation method. In our case, additional complications arise owing to vectorial and nonseparable character of the problem. So we need a 3-D vectorial PE describing paraxial wave propagation along a smoothly curved waveguide axis and admitting appropriate boundary conditions (BC’s) on the tunnel walls.

Computational efficiency of the vectorial PE has been demonstrated recently in [17], [18] where realistic problems of EM propagation and scattering were solved on a modest desktop computer. In our case, an essential modification of the ordinary vectorial PE is required to adapt it to the curved propagation line. A reliable way to do that is based on the rigorous asymptotic solution [12] described in Section II. As has been pointed out in [19], the asymptotic series of the adiabatic mode theory can be rearranged by including the first-order correction into the leading term of the asymptotic expansion. Such a rearrangement yields a new two-component vectorial PE describing diffraction, attenuation and depolarization of arbitrary paraxial EM wave packets in smoothly nonuniform oversized lossy waveguides, including exponentially small effects of nonadiabatic mode conversion [20]. This is the main contents of Section III. In order

Manuscript received August 31, 1999; revised June 19, 2000. This work was supported in part by the Deutsche Forschungsgemeinschaft under Grant La 484/19-1.

A. V. Popov is with the Institute of Terrestrial Magnetism, Ionosphere and Radio Wave Propagation, Russian Academy of Sciences, Troitsk, Moscow, 142190 Russia (e-mail: popov@izmiran.rssi.ru).

N. Y. Zhu is with the Institut für Hochfrequenztechnik, Universität Stuttgart, D-70550 Stuttgart, Germany (e-mail: zhu@ihf.uni-stuttgart.de).

Publisher Item Identifier S 0018-926X(00)09355-8.

not to overload the paper with cumbersome derivations we assume from the beginning Leontovich BC's to be imposed on the waveguide walls. The applicability of the impedance BC's for curved material surfaces has been studied in [13] and [21].

For simple tunnel profiles the vectorial PE can be solved analytically and the solution can be used for validation purposes (Section IV). In the general case, numerical solution of the PE is obtained using the Crank–Nicolson finite-difference/finite-element (FD/FE) scheme with a sparse matrix solver (cf. [18], [22]) or FD splitting techniques [22]. In the immediate vicinity of the radiation source, the PE does not properly describe the wave field distribution and is to be replaced with another approximation. In order to provide correct initial values for PE integration, we make use of a GO based computer code [23] calculating geometrical reflection of the primary dipole radiation from the impedance surfaces. This combination enables one to study radio wave propagation in the complete range of interest (Section V). Finally, Section VI summarizes the main points of this work.

## II. ADIABATIC MODES OF CURVED EM WAVEGUIDES

Consider a smoothly nonuniform waveguide (Fig. 1). Generally, its axis  $\bar{r}_0(s)$  is a space curve,  $s$  being the arc length. We introduce a local Cartesian frame  $(y, z)$  in the waveguide cross section  $s = \text{Const}$ :  $\bar{r}(s, y, z) = \bar{r}_0(s) + y\bar{e}_y + z\bar{e}_z$  with  $\bar{e}_y = \bar{m} \cos \theta - \bar{b} \sin \theta$ ,  $\bar{e}_z = \bar{m} \sin \theta + \bar{b} \cos \theta$  where  $\bar{m}$  and  $\bar{b}$  denote, respectively, the principal normal and binormal of the waveguide axis  $\bar{r}_0(s)$ . Rotation angle  $\theta$  is related to the torsion  $\tau$  of the axis via  $\theta = \theta_0 + \int_0^s \tau(s) ds$ . The Lamé coefficients of the system  $(s, y, z)$  are  $h, 1, 1$  with  $h = 1 - (y \cos \theta + z \sin \theta) / \rho(s)$ , where  $\rho(s)$  denotes the curvature radius of the waveguide axis  $\bar{r}_0(s)$ —cf. [16].

Let us summarize the physical considerations mentioned in the Introduction.

- 1) We are interested in high-frequency propagation when the wavelength  $\lambda$  is small compared with the waveguide diameter  $D$  (oversized waveguide).
- 2) As a rule, dominant propagation modes have small Brillouin angles with respect to the waveguide axis.
- 3) Relative axis curvature [ratio between the diameter  $D$  and the curvature radius  $\rho(s)$ ] is usually very small;
- 4) Leontovich impedance BC  $\bar{n} \times \bar{E} = -Z\bar{n} \times (\bar{n} \times \bar{H})$  can be used as an approximation of the wall electrical properties, cf. [13], [21].

These restrictions can be formalized by introducing a small parameter  $\nu = \sqrt{D/L} \ll 1$  and assuming  $\lambda/D = O(\nu)$ ,  $L/\rho(s) = O(1)$ . Here,  $L \gg D$  is a characteristic scale of the longitudinal nonuniformity (these order relations are usually satisfied for the VHF/UHF band while the precise definition of the parameters  $D, L$  is not important as they do not appear in the final equations). Diffraction processes in such nonuniform waveguides are governed by the Fresnel number  $D^2/\lambda L = O(\nu) \ll 1$  and another dimensionless parameter, which can be called the Fock number  $\sqrt{D^3/\lambda^2 L} = O(1)$ , as it appears implicitly in Fock's classical study of short wave diffraction by a convex cylinder [13, chs. 7-9]. In that case, the cylinder radius  $\rho(s)$  stands for the longitudinal scale  $L$  while the transverse

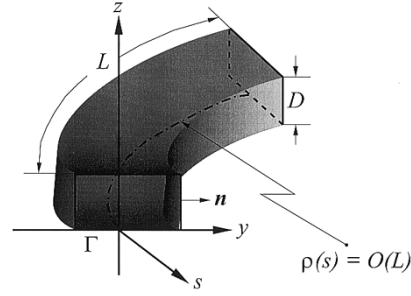


Fig. 1. A curved tunnel

scale  $D \sim (\rho/k^2)^{1/3}$  determines the boundary layer thickness where the creeping waves are formed ( $k = 2\pi/\lambda$  is the wavenumber). Corresponding order relations  $\nu = kD^2/L \sim (k\rho)^{-1/3} \ll 1$ ,  $\sigma = (k^2 D^3/L)^{1/2} \sim 1$  allow for a simple and versatile field description in terms of the parabolic equation. A similar boundary layer arises in the case of the whispering gallery mode [11], [16]. In our case, due to the waveguide boundary conditions, a more sofisticated vectorial propagation mode emerges, but the above order relations still hold.

In order to construct an asymptotic solution of the considered propagation problem we introduce scaled variables  $\xi = s/L$ ,  $\eta = y/D$ ,  $\zeta = z/D$ ;  $\kappa(\xi) = L/\rho(s)$  and rewrite the governing Maxwell equations (time dependence  $\exp(j\omega t)$  is used in this work)

$$\text{rot } \bar{H} = jk\bar{E}, \quad \text{rot } \bar{E} = -jk\bar{H} \quad (1)$$

putting the electric and the magnetic fields together in a six-component vector  $\bar{\Pi} = (hE_\xi, E_\eta, E_\zeta, hH_\xi, H_\eta, H_\zeta)^T$  (cf. [12]). Direct substitution yields a six-component PDE

$$\begin{aligned} \nu^3 \bar{L} \frac{\partial \bar{\Pi}}{\partial \xi} + \nu \left[ \bar{M}_0 + (1 - h^2) \bar{M}_1 \right] \frac{\partial \bar{\Pi}}{\partial \eta} \\ + \nu \left[ \bar{N}_0 + (1 - h^2) \bar{N}_1 \right] \frac{\partial \bar{\Pi}}{\partial \zeta} \\ = -j\sigma h \bar{R} \bar{\Pi}. \end{aligned} \quad (2)$$

Here,  $\sigma = \sqrt{k^2 D^3/L}$ ;  $\bar{L}$ ,  $\bar{M}_0$ ,  $\bar{M}_1$ ,  $\bar{N}_0$ , and  $\bar{N}_1$ , are constant diagonal block matrices, and  $\bar{R}$  is an antidiagonal block matrix

$$\begin{aligned} \bar{L} &= \text{diag} [\bar{l}, -\bar{l}], \quad \bar{M}_0 = \text{diag} [\bar{m}_0, -\bar{m}_0] \\ \bar{M}_1 &= \text{diag} [\bar{m}_1, -\bar{m}_1], \quad \bar{N}_0 = \text{diag} [\bar{n}_0, -\bar{n}_0] \\ \bar{N}_1 &= \text{diag} [\bar{n}_1, -\bar{n}_1], \quad \bar{R}_0 = \begin{pmatrix} \bar{0} & \bar{I} \\ \bar{I} & \bar{0} \end{pmatrix} \\ \bar{l} &= \begin{pmatrix} 1 & 0 & 0 \\ 0 & 1 & 0 \\ 0 & 0 & 1 \end{pmatrix}, \quad \bar{I} = \begin{pmatrix} 0 & 0 & 0 \\ 0 & 0 & -1 \\ 0 & 1 & 0 \end{pmatrix} \\ \bar{m}_0 &= \begin{pmatrix} 0 & 0 & 1 \\ 0 & 0 & 0 \\ -1 & 0 & 0 \end{pmatrix}, \quad \bar{m}_1 = \begin{pmatrix} 0 & 0 & -1 \\ 0 & 0 & 0 \\ 0 & 0 & 0 \end{pmatrix} \\ \bar{n}_0 &= \begin{pmatrix} 0 & -1 & 0 \\ 1 & 0 & 0 \\ 0 & 0 & 0 \end{pmatrix}, \quad \bar{n}_1 = \begin{pmatrix} 0 & 1 & 0 \\ 0 & 0 & 0 \\ 0 & 0 & 0 \end{pmatrix}. \end{aligned}$$

In this concise dimensionless notation of Maxwell's equations, our small parameter  $\nu$  appears explicitly, making clear the asymptotic character of the problem. It is easily seen that (2) represents a singularly perturbed system and cannot be solved by straightforward expansion in powers of  $\nu$ . A good guess is to allow the solution to oscillate along the waveguide axis as  $\exp[-j\sigma\Phi(\xi)/\nu^3]$  and to assume the lateral derivatives  $\partial\bar{\Pi}/\partial\eta$ ,  $\partial\bar{\Pi}/\partial\zeta$  being of order of unity in virtue of the above agreement 2) to consider low-order modes with small Brillouin angles  $\beta = O(\nu)$ . That suggests the following asymptotic Ansatz:

$$\bar{\Pi} = \bar{U} \exp(-j\sigma\Phi/\nu^3) \quad (3)$$

where the eikonal  $\Phi$ , in general, is a second-order polynomial of  $\nu$  and the vector amplitude  $\bar{U}(\xi, \eta, \zeta)$  is sought as an asymptotic series in powers of  $\nu$

$$\Phi(\xi) = \Phi_0 + \nu\Phi_1 + \nu^2\Phi_2, \quad \bar{U} = \sum_{i=0}^{\infty} \nu^i \bar{U}_i(\xi, \eta, \zeta). \quad (4)$$

It is assumed that the vector amplitudes  $\bar{U}_i$  are slowly varying functions—true for low-order modes with  $\beta = O(\nu)$ . After substituting (3) into PDE (2) and equating coefficients of like powers of  $\nu$ , we get a sequence of linear algebraic equations for the vector amplitudes  $\bar{U}_n$

$$\begin{aligned} \bar{S}\bar{U}_i &= \bar{F}_i, \quad i = 0, 1, \dots; \quad \bar{S} = \bar{R} - \Phi'_0(\xi)\bar{L} \\ \bar{F}_i &= \frac{j}{\sigma} \left( \bar{M}_0 \frac{\partial}{\partial\eta} + \bar{N}_0 \frac{\partial}{\partial\zeta} \right) \bar{U}_{i-1} \\ &+ \left[ \kappa(\eta\cos\theta + \xi\sin\theta)\bar{R} + \Phi'_2(\xi)\bar{L} \right] \bar{U}_{i-2} \\ &+ \frac{j}{\sigma} \left[ \bar{L} \frac{\partial}{\partial\xi} + 2\kappa(\eta\cos\theta + \xi\sin\theta) \right. \\ &\cdot \left. \left( \bar{M}_1 \frac{\partial}{\partial\eta} + \bar{N}_1 \frac{\partial}{\partial\zeta} \right) \right] \bar{U}_{i-3}, \quad 0 \leq i \leq 4. \end{aligned} \quad (5)$$

The homogeneous zero-order equation has a nontrivial solution only if  $\det\bar{S} = 0$ , which gives  $\Phi_0(\xi) = \xi$ ,  $\bar{U}_0 = u_0\bar{a} + v_0\bar{b}$ , where  $\bar{a} = (0, 1, 0, 0, 0, 1)^T$ ,  $\bar{b} = (0, 0, 1, 0, -1, 0)^T$  are two annulling eigenvectors of the reduced matrix  $\bar{S} = \bar{R} - \bar{L}$ . Solvability conditions of the next nonhomogeneous equation ( $i = 1$ ) (cf. [10], [12]) result in  $\Phi_1(\xi) \equiv 0$ ,  $\bar{U}_1 = u_1\bar{a} + v_1\bar{b} + \bar{f}_1$

$$\bar{f}_1 = \frac{j}{\sigma} \left( -\frac{\partial u_0}{\partial\eta} - \frac{\partial v_0}{\partial\zeta}, 0, 0, \frac{\partial v_0}{\partial\eta} - \frac{\partial u_0}{\partial\zeta}, 0, 0 \right)^T. \quad (6)$$

Coefficients  $u_i(\xi, \eta, \zeta)$ ,  $v_i(\xi, \eta, \zeta)$  are at this stage arbitrary scalar functions. Clearly, the zero-order approximation yields a purely transverse electromagnetic field, while the first-order correction introduces a small longitudinal component  $\nu\bar{f}_1$ .

In order to complete constructing the leading term of the asymptotic solution (3) and to find the first-order corrections, one has to determine the unknown amplitude functions  $\bar{u}_i(\xi, \eta, \zeta)$  and  $\bar{v}_i(\xi, \eta, \zeta)$ ,  $i = 0, 1$  in (6). They satisfy the following differential equations in vector notation for  $\bar{w}_i = (u_i, v_i)^T$ :

$$\begin{aligned} \Delta_{\perp} \bar{w}_i - 2\sigma^2 [\gamma + \kappa(\eta\cos\theta + \xi\sin\theta)] \bar{w}_i &= 2j\sigma \frac{\partial \bar{w}_{i-1}}{\partial\xi} \\ i = 0, 1 \end{aligned} \quad (7)$$

following from the solvability conditions for the subsequent amplitude vectors  $\bar{U}_2, \bar{U}_3$  [12]. Here,  $\Delta_{\perp} = (\partial^2/\partial\eta^2) + (\partial^2/\partial\zeta^2)$  and  $\gamma(\xi) = \Phi'_2(\xi)$ . It is implied that  $\bar{w}_{-1} \equiv 0$ , so the zero-order PDE is homogeneous.

At the boundary contour  $\Gamma$  of the waveguide cross section, conditions to be met by  $\bar{w}_i$  arise from substituting the Ansatz (3) into the impedance BC:  $\bar{n} \times \bar{E} = -Z\bar{n} \times (\bar{n} \times \bar{H})$ . Equating the terms of the same order of  $\nu$  we get

$$\bar{w}_0|_{\Gamma} = 0, \quad \bar{w}_1|_{\Gamma} = \frac{j}{\sigma} \bar{T}_0 \bar{G} \bar{T}_0 \frac{\partial \bar{w}_0}{\partial n} \Big|_{\Gamma} \quad (8)$$

with

$$\bar{T}_0 = \begin{pmatrix} n_y & n_z \\ n_z & -n_y \end{pmatrix}, \quad \bar{G} = \begin{pmatrix} 1/Z & 0 \\ 0 & Z \end{pmatrix}.$$

Here,  $\bar{n} = (n_y, n_z)$  is the unit normal to  $\Gamma$  and  $Z$  is the impedance, not necessarily uniform, of the tunnel walls. For a wall material with relative permittivity  $\epsilon_r$  and conductivity  $\sigma_0$  there is approximately  $Z = 1/\sqrt{\epsilon_r - j60\lambda\sigma_0}$  (see [13], [21]).

As both components of the zero-order vector amplitude  $\bar{w}_0 = (u_0, v_0)^T$  satisfy identical PDE (7) and BC (8), they are proportional to a single scalar eigenfunction of the Dirichlet boundary value problem  $w_0|_{\Gamma} = 0$ . The corresponding eigenvalue  $\gamma_{mn}(s)$  gives a small index-dependent correction to the zero-order eikonal:  $\Phi_2(\xi) = \int \gamma_{mn}(\xi) d\xi$ . Once  $w_{mn}(s, y, z)$  and  $\gamma_{mn}(s)$  are found [both depend on the longitudinal variable  $s = L\xi$  via curvature radius  $\rho(s)$  and torsion angle  $\theta(s)$ ] the leading term of (3) is determined but for a normalizing polarization vector:  $\bar{w}_0(s, y, z) = (A, B)^T w_{mn}(s, y, z)$ . Its components  $A(s), B(s)$ , from the solvability condition of the inhomogeneous boundary problem for  $\bar{w}_1(s, y, z)$ , are coupled via a pair of ODE's [12]

$$\frac{dA}{ds} = P_{11}A + P_{12}B, \quad \frac{dB}{ds} = P_{12}A + P_{22}B \quad (9)$$

coefficients  $P_{ij}$  being functionals of the impedance  $Z$

$$\begin{aligned} P_{11} &= -\frac{1}{2k^2} \int_{\Gamma} (n_y^2/Z + n_z^2Z) \left( \frac{\partial w_{mn}}{\partial n} \right)^2 d\Gamma \\ P_{12} &= -\frac{1}{2k^2} \int_{\Gamma} n_y n_z (1/Z - Z) \left( \frac{\partial w_{mn}}{\partial n} \right)^2 d\Gamma \\ P_{22} &= -\frac{1}{2k^2} \int_{\Gamma} (n_y^2Z + n_z^2/Z) \left( \frac{\partial w_{mn}}{\partial n} \right)^2 d\Gamma. \end{aligned} \quad (10)$$

They determine attenuation and depolarization of the propagating waveguide mode due to absorption and coupling of the electric field components in the waveguide wall material. Equation (10) shows that generically these two effects become more significant with growing indices  $m, n$ .

### III. VECTORIAL PE FOR A CURVED TUNNEL

Asymptotic analysis of Section II yields a series of low-order, minimum absorption modes of an arbitrarily shaped, smoothly nonuniform oversized waveguide. Their propagation characteristics can be calculated explicitly for arbitrary cross-sectional shape and material properties. Unexpectedly simple analytical formulas (10) can be used as a basis to predict propagation losses in realistic tunnel environments. However, the principal drawbacks of modal theory still remain. First, in an oversized waveguide several modes can have almost identical attenuation,

so it is not easy to foresee which will be dominant. Second, in many applications, such as mobile cellular communication, one is interested in prediction of radio wave propagation not only over large distances but also at intermediate ranges. For this purpose, too many modes would be necessary to adequately describe strong field variations inherited from the near field multiray structure. Finally, practical applications require more realistic modeling including local inhomogeneities created by traffic and technical constructions. In this case, using modal theory becomes cumbersome and impractical. This motivated us to look for an alternative description of the wave field in tunnel-like environments.

Such an alternative approach is suggested by the recursive equations (7) reminiscent of the well-known parabolic wave equation [13]–[15]. Of course, (7) is not a PE; just a recursive two-dimensional PDE, because the functions in the right- and left-hand sides are different. However, we can derive an approximate vectorial PE by considering a partial sum of the power series (4). Having confined ourselves to the first two terms and denoting

$$\bar{w} = \bar{w}_0 + \nu \bar{w}_1$$

we obtain from (7), as a linear combination of the equations governing  $\bar{w}_0$  and  $\bar{w}_1$ , the following relationship:

$$\Delta_{\perp} \bar{w} - 2\sigma^2 [\gamma + \kappa(\eta \cos \theta + \zeta \sin \theta)] \bar{w} = 2j\nu\sigma \frac{\partial \bar{w}_0}{\partial \xi}.$$

By neglecting the second-order terms, this equation becomes self-consistent

$$\Delta_{\perp} \bar{w} - 2\sigma^2 [\gamma + \kappa(\eta \cos \theta + \zeta \sin \theta)] \bar{w} \approx 2j\nu\sigma \frac{\partial \bar{w}}{\partial \xi}.$$

To eliminate the range- and index-dependent eigenvalue  $\gamma = \gamma_{mn}(\xi)$ , consider next a modified unknown vector  $\bar{W} = (U, V)$  defined as  $\bar{W} = \bar{w} \exp(-j\sigma\nu^{-1} \int \gamma d\xi)$ . Immediately, a governing equation for  $\bar{W}$  comes up

$$2j\nu\sigma \frac{\partial \bar{W}}{\partial \xi} \approx \Delta_{\perp} \bar{W} - 2\kappa\sigma^2 (\eta \cos \theta + \zeta \sin \theta) \bar{W} \quad (11)$$

a partial differential equation of “parabolic” type. A remarkable feature is its independence of the mode number  $(m, n)$ , which means that any superposition of adiabatic low-order waveguide modes satisfies (11) to the accuracy  $O(\nu^2)$ . Being based on the rigorous asymptotic analysis [12], this vectorial PE can be used as a reliable tool for field calculations in smoothly nonuniform oversized EM wavguides.

In accordance with (3)–(6), vector function  $\bar{W}$  is related to the tangential electric field in the tunnel cross section  $\bar{E}_{\perp} = (E_{\eta}, E_{\zeta})^T$  via  $\bar{E}_{\perp} = \bar{W} \exp(-j\sigma\xi/\nu^3) + O(\nu^2)$ . Using the terminology of radio wave propagation theory [13],  $\bar{W}(s, y, z)$  can be called the attenuation function which describes the complex wave amplitude of the approximately plane wave  $\exp(-jks)$  propagating along the smoothly curved waveguide axis. A similar procedure transforms the recursive relation (8) to an approximate BC for  $\bar{W}$  to be met at the cross section contour  $\Gamma$ . As it was stated in Section II, the above equations do not depend on the precise definition of the scaling parameters  $D$  and  $L$  that served just to clarify the asymptotic character of the problem. Returning to the original

physical variables  $(s, y, z)$ , the two-component vectorial PE for paraxial EM waves in a wide smoothly curved tunnel now reads  $\bar{E}_{\perp} = (E_y, E_z)^T = \bar{W} \exp(-jks)$

$$2kj \frac{\partial \bar{W}}{\partial s} = \frac{\partial^2 \bar{W}}{\partial y^2} + \frac{\partial^2 \bar{W}}{\partial z^2} - 2k^2 \frac{y \cos \theta(s) + z \sin \theta(s)}{\rho(s)} \bar{W}. \quad (12)$$

The tangential electric field components  $E_y, E_z$  are weakly coupled through a matrix BC

$$\bar{W}|_{\Gamma} = \frac{j}{k} \bar{T}_0 \bar{G} \bar{T}_0 \frac{\partial \bar{W}}{\partial n} \Big|_{\Gamma}. \quad (13)$$

This boundary value problem gives a full wave description of paraxial EM propagation along the curved waveguide axis. Equation (12) accounts for transversal diffusion of the vector wave amplitude  $\bar{W}(s, y, z)$  over the approximate plane wave fronts  $s = \text{Const}$  [14], whereas the matrix BC (13) governs the effects of grazing angle reflection, selective mode absorption and depolarization in the curved waveguide walls. Depending on the spectral contents, its solution can represent a wide variety of the wave fields evolving from sharp “ray-like” interference patterns inherited from GO in the vicinity of the radiation source to a smooth “mode-like” cross-sectional field distribution at large ranges where a small number of modes become dominant (see Section V).

In view of the approximate nature of (12) and (13), it is necessary to look at the uniqueness of their solution at this stage. Generalizing the well-known technique developed for scalar PEs (e.g., [24]), consider the power  $P(s)$  passing through the tunnel cross section  $S$

$$P(s) = \int_S |\bar{W}|^2 dS = \int_S (|U|^2 + |V|^2) dS.$$

On use of (12) and (13), its evolution with varying range  $s$  can be expressed in terms of the boundary values of the transversal field divergence and vortex

$$\begin{aligned} \frac{dP(s)}{ds} = & -\frac{1}{k^2} \int_{\Gamma} \left[ \text{Re.} \left( \frac{1}{Z} \right) \left| \frac{\partial U}{\partial y} + \frac{\partial V}{\partial z} \right|^2 \right. \\ & \left. + \text{Re.} Z \left| \frac{\partial U}{\partial z} - \frac{\partial V}{\partial y} \right|^2 \right] d\Gamma. \end{aligned} \quad (14)$$

For passive tunnel walls there is always  $\text{Re.} Z \geq 0$  and, hence,  $\text{Re.}(1/Z) \geq 0$ . This implies that the power  $P(s)$  carried by the one-way propagating wave field  $\bar{W}$  never increases. Therefore, it turns out immediately that the boundary value problem (12), (13) is uniquely solvable. In fact, let  $\bar{W} = \bar{W}_1 - \bar{W}_2$  be the difference between two possible solutions corresponding to the same initial value. Evidently,  $\bar{W}(s, y, z)$  satisfies the PE (12), and  $P(0) = 0$ . Thus, in virtue of (14), its energy flow equals identically to zero  $P(s) \equiv 0$ . This, in turn, shows that  $U \equiv 0$ ,  $V \equiv 0$ , i.e.,  $\bar{W}_1 \equiv \bar{W}_2$ , which means the uniqueness of the solution.

We note that (12) is a vectorial counterpart of the scalar PEs describing creeping and whispering gallery waves [13], [16] and includes, as a special case [for a straight tunnel with  $\rho(s) \equiv \infty$ ], the vectorial version of the Leontovich–Fock PE used in [17]. Being asymptotically equivalent to the rigorous adiabatic mode theory of Section II at the ranges  $s = O(L)$ , it opens an easy and

reliable way to model EM wave propagation in realistic weakly nonuniform tunnels. For larger distances or greater waveguide axis curvature, PE reveals exponentially small (in  $\nu$  parameter) nonadiabatic effects, such as residual mode conversion after having passed an analytically smooth transition between two regular waveguides (cf. [20]).

#### IV. VALIDATION, COMPARISON, APPLICABILITY

The main purpose of this section is validation of our approach by comparison with the published results on radio wave propagation in tunnels. As most estimates have been obtained for rectangular tunnel profiles, we will consider this simplest case in more detail. This analysis will also clarify the relation between the vectorial PE and the adiabatic mode theory of Section II.

Let the tunnel cross section  $S$  be a rectangle  $|y| \leq a$ ,  $0 \leq z \leq b$ . In this case,  $n_y$  and  $n_z$ , two components of the outward pointing normal on  $\Gamma$ , vanish alternatively at the vertical side walls  $y = \pm a$ , horizontal floor  $y = 0$  and ceiling  $y = b$ , so the impedance matrix  $\bar{T}_0 \bar{G} \bar{T}_0$  becomes diagonal. Therefore, transversal electric field components  $W_y = U(s, y, z)$  and  $W_z = V(s, y, z)$  in the orthogonal frame  $(y, z)$  turn out to be completely decoupled. This allows one to find two independent series of adiabatic modes corresponding to horizontal or vertical  $\bar{E}_\perp$ .

Consider for example vertical  $\bar{E}_\perp$  polarization described by the  $V$  component of the attenuation function  $\bar{W}$ . As follows from (12), (13), it satisfies the respective scalar PE

$$2jk \frac{\partial V}{\partial s} = \frac{\partial^2 V}{\partial y^2} + \frac{\partial^2 V}{\partial z^2} - 2k^2 \frac{y \cos \theta(s) + z \sin \theta(s)}{\rho(s)} V \quad (15)$$

with the third-kind BCs

$$\left[ V \pm \frac{Z_\parallel}{jk} \frac{\partial V}{\partial y} \right]_{y=\pm a} = 0, \quad \left[ V \mp \frac{1}{jk Z_\perp} \frac{\partial V}{\partial z} \right]_{z=0, b} = 0 \quad (16)$$

determined, accordingly, by the characteristic impedances:  $Z_\parallel$  of the side walls and  $Z_\perp$  of the the tunnel floor and ceiling (we consider them generally to be different).

For  $\rho = \text{Const}$ ,  $\theta = \text{Const}$ , low-order modes of such a waveguide can be obtained by separation of variables:

$$V(s, y, z) = \Psi(y)\Xi(z)\exp(P_{22}s) \quad (17)$$

(we choose the notation consistent with Section II). Standard procedure yields the corresponding eigenfunctions expressed in terms of Airy functions [16], [25]

$$\begin{aligned} \Psi(y) &= C_1 \text{Ai}(t) + C_2 \text{Bi}(t) \\ \Xi(z) &= D_1 \text{Ai}(x) + D_2 \text{Bi}(x). \end{aligned} \quad (18)$$

Here, new variables  $t = t_0 + gy/a$ ,  $x = x_0 + pz/b$  are introduced;  $q = (2k^2 \cos \theta/\rho)^{1/3}a$ ,  $p = (2k^2 \sin \theta/\rho)^{1/3}b$  are dimensionless parameters, while  $t_0$  and  $x_0$  are constant eigenvalues to be found from BC (16).

Inserting (18) into (16), one obtains the following transcendental equations:

$$\begin{aligned} \frac{[\text{Bi}(t^+) + Q\text{Bi}'(t^+)]}{[\text{Ai}(t^+) + Q\text{Ai}'(t^+)]} \frac{[\text{Ai}(t^-) - Q\text{Ai}'(t^-)]}{[\text{Bi}(t^-) - Q\text{Bi}'(t^-)]} &= 1 \\ Q &= \frac{qZ_\parallel}{jka} \\ \frac{[\text{Bi}(x^+) + P\text{Bi}'(x^+)]}{[\text{Ai}(x^+) + P\text{Ai}'(x^+)]} \frac{[\text{Ai}(x_0) - P\text{Ai}'(x_0)]}{[\text{Bi}(x_0) - P\text{Bi}'(x_0)]} &= 1 \\ P &= \frac{q}{jkaZ_\perp} \end{aligned} \quad (19)$$

with  $t^\pm = t_0 \pm q$ ,  $x^+ = x_0 + p$ , to be solved for  $t_0$ ,  $x_0$ . They are similar to those obtained in a particular case ( $\theta = 0$ ,  $Z_\perp = 0, \infty$ ) by Mahmoud and Wait [7] and become identical for the fundamental mode thoroughly studied in [7]. Equations (19) can be solved numerically, which enables one to calculate the complex exponent

$$\begin{aligned} P_{22} &= \frac{1}{2jk} \left( \frac{q^2}{a^2} t_0 + \frac{p^2}{b^2} x_0 \right) \\ &= -jk \frac{t_0(\cos \theta)^{2/3} + x_0(\sin \theta)^{2/3}}{(2k^2 \rho^2)^{1/3}} \end{aligned} \quad (20)$$

determining phase velocity and attenuation of the waveguide mode, as well as its cross-sectional pattern via equations (18). To illustrate the effects of curvature and torsion we include a series of transversal field patterns in a rectangular waveguide with the dimensions and wall electric properties of a typical road tunnel (Fig. 2).

It is well known that the tunnel axis curvature causes the field concentration near the concave side wall. Surprisingly, even frequently encountered small values of tunnel curvature give a very strong concentration effect forming the whispering gallery mode [11] completely detached from the convex inner wall—compare Fig. 2(a) and (b). In the general case of nonplanar 3-D axis curve, its torsion causes local tilts of the waveguide cross section, which can also change the modal field pattern. As one could foresee, for tunnel environments this effect is almost negligible: we can notice a difference solely for unrealistically high tilt angles like  $\theta = 45^\circ$ —compare Fig. 2(b) and (c). As this effect depends upon the cross sectional shape and dimensions of the waveguide, we mention it, bearing in mind possible applications of the proposed theory to other oversized guiding structures.

As the dimensionless constants  $qZ_\parallel/ka$  and  $p/kbZ_\perp$  are usually small, explicit approximate formulae can be obtained using perturbation theory. The zero-order approximation

$$\begin{aligned} \text{Ai}(t^-)\text{Bi}(t^+) - \text{Bi}(t^-)\text{Ai}(t^+) &= 0 \\ \text{Ai}(x_0)\text{Bi}(x^+) - \text{Bi}(x_0)\text{Ai}(x^+) &= 0 \end{aligned} \quad (21)$$

agrees with the results of Section II (cross-sectional field distribution in the leading term of the asymptotic solution is found from a Dirichlet boundary value problem while the effects of the wall impedances appear only in the higher-order terms). Furthermore, if  $t^+ \gg 1$  (actually,  $t^+ \geq 3$ ) the first term in the upper line of (21), containing  $\text{Bi}(t^+)$ , dominates and it simplifies to  $\text{Ai}(t^-) = 0$ . Its evident solution is  $t^- = -t_m$ ,  $t_0 = q - t_m$

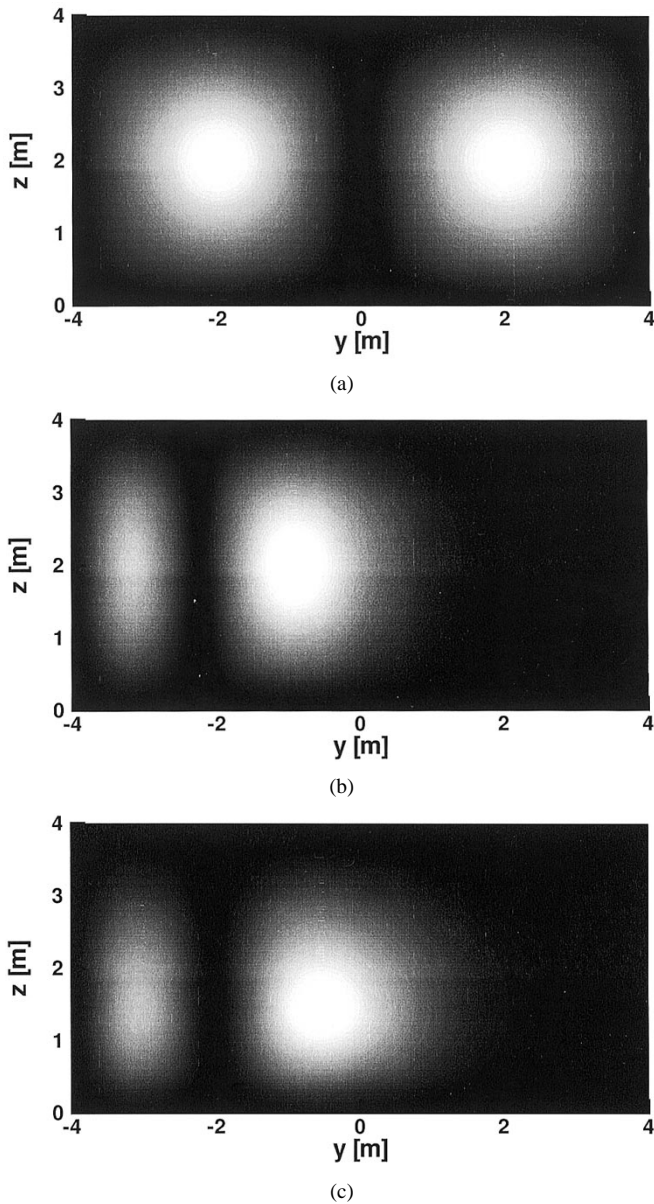


Fig. 2.  $|V(y, z)|$  of the  $2 \times 1$  mode in rectangular tunnels with  $\epsilon_r = 5.5$  and  $\sigma_0 = 0.03$  S/m at 950 MHz with the brightness proportional to the normalized amplitude. (a)  $\rho = \infty$  m,  $\theta = 0^\circ$ . (b)  $\rho = 800$  m,  $\theta = 0^\circ$ . (c)  $\rho = 800$  m,  $\theta = 45^\circ$ .

where  $t_m$ ,  $m = 1, 2, \dots$  are the negative roots of the Airy function—see [16], [25]. In this case, the horizontal eigenfunction is proportional to

$$\Psi(y) \sim \text{Ai} \left[ -t_m + q \left( 1 + \frac{y}{a} \right) \right]. \quad (22)$$

Physically, that means that the wave field is detached from the convex right waveguide wall  $y = a$  due to strong curvature effects and a purely whispering gallery wave [11] is formed near the concave wall  $y = -a$ .

In the opposite case of very small axis curvature, parameter  $t_0$  becomes large and, after replacing in (18) the Airy functions with their WKB asymptotics (see [16], [25]), an approximate solution arises

$$\Psi(y) \sim \sin \left[ (\tau - \tau^+) \left( 1 + \frac{5}{72\tau\tau^+} \right) \right] \quad (23)$$

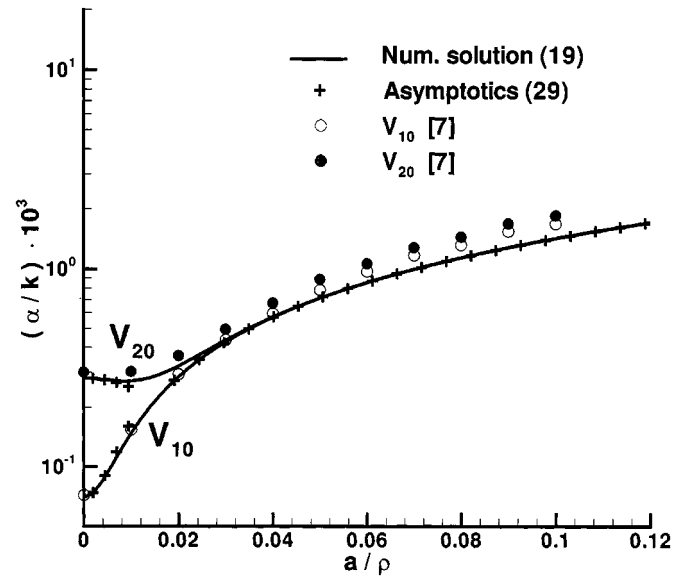


Fig. 3. Attenuation rate for  $V_{10}$  and  $V_{20}$  modes in a rectangular tunnel with electrically perfectly conducting ceiling and floor ( $f = 1000$  MHz, tunnel width  $2a = 2.133$  m; wall parameters:  $\epsilon_r = 10$ ,  $\sigma_0 = 0.01$  S/m) as a function of relative curvature  $a/\rho$ . Solid lines: numerical solution of the transcendental equation (19), crosses: asymptotic formulas (29); circles: numerical results of [7] for  $\text{LSM}_{0,1} \equiv V_{10}$  and  $\text{LSM}_{0,2} \equiv V_{20}$  modes.

with  $\tau = (2/3)(-t)^{3/2}$ ,  $\tau^+ = (2/3)(-t^+)^{3/2}$ . Evidently, function (23) vanishes at  $y = a$ . Imposing similar BC  $\Psi(-a) = 0$  at the left-side wall  $y = -a$ , one obtains instead of (21) a simplified transcendental equation

$$\sin \left[ 2q(-t_0)^{1/2} \left( 1 - \frac{1}{24} \frac{q^2}{t_0^2} \right) \left( 1 - \frac{5}{32t_0^3} \right) \right] = 0 \quad (24)$$

with the approximate solution

$$t_0 \approx - \left( \frac{\pi m}{2q} \right)^2 + 5 \left( \frac{q}{\pi m} \right)^4 - \frac{1}{3} \frac{q^4}{\pi^2 m^2}, \quad m = 1, 2, \dots \quad (25)$$

Substitution into (23) yields

$$\Psi(y) \approx \sin \left[ \frac{\pi m}{2} \left( 1 - \frac{y}{a} \right) \right] + O(q) \quad (26)$$

a simple straight waveguide mode with a small correction proportional to the axis curvature to the power 1/3. A similar approximation is valid for the vertical eigenfunctions

$$x_0 \approx - \frac{\pi^2 n^2}{p^2}, \quad \Xi(z) \approx \sin \frac{\pi n}{b} z, \quad n = 1, 2, \dots \quad (27)$$

as the torsion effects are usually very small. Perturbation theory applied to the exact transcendental equation (19) yields small corrections to the eigenvalues  $t_0$ ,  $x_0$  due to the surface impedances  $Z_{\parallel}$ ,  $Z_{\perp}$ , which results in the following approximate formula:

$$P_{22} \approx - \frac{Z_{\parallel}}{\rho} \frac{dt_0}{dq} - \frac{\lambda^2 n^2}{2b^3 Z_{\perp}} \quad (28)$$

being in full agreement with the straightforward evaluation of the contour integral (10) of Section II. In the above mentioned limiting cases of the whispering gallery or of the almost straight waveguide modes, the corresponding approximate formulae for

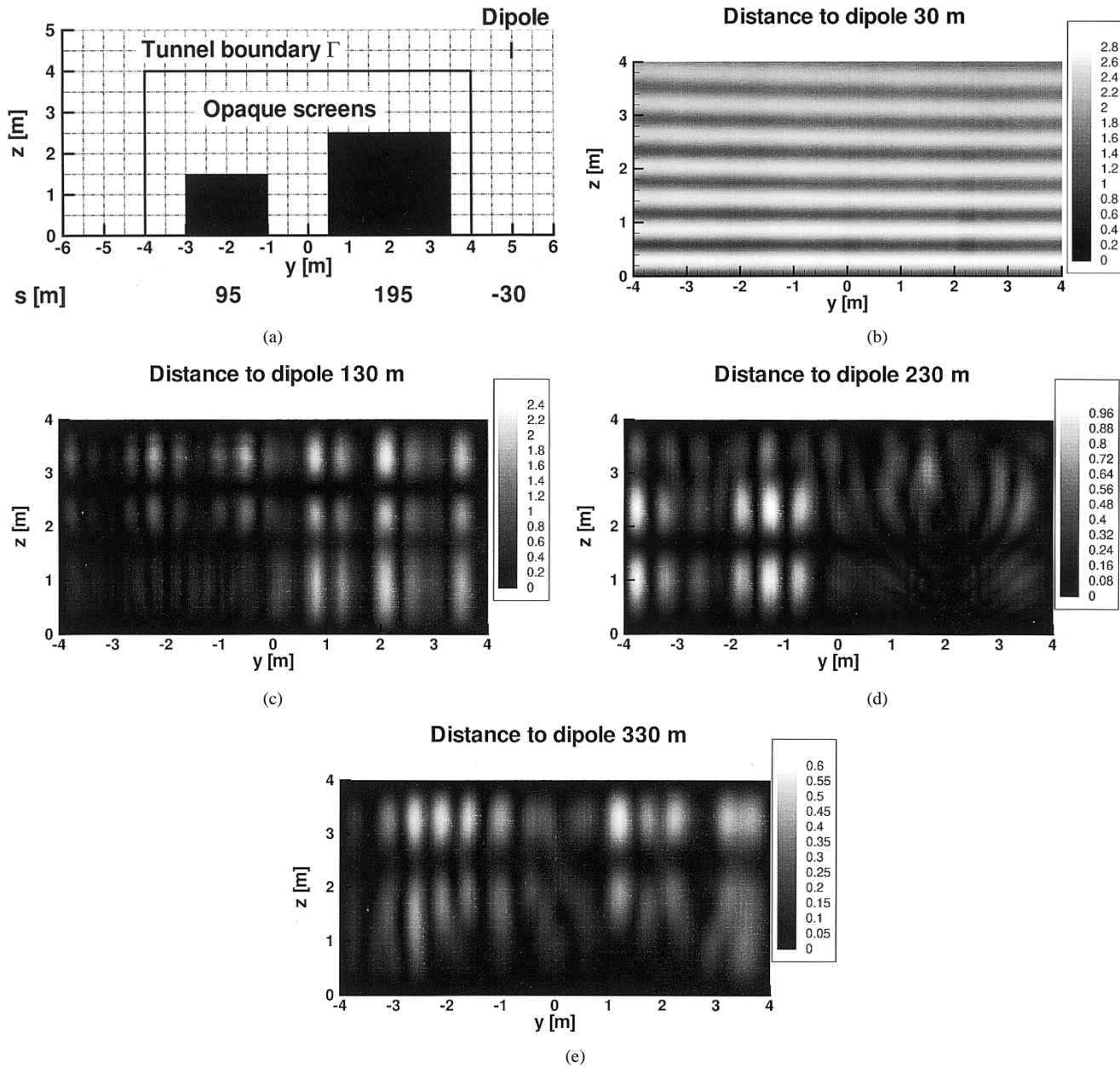


Fig. 4.  $|V(y, z)|$  in a rectangular tunnel with traffic obstructions at different distances to a vertical half-wavelength dipole placed 30 m outside the tunnel entrance ( $f = 1.8$  GHz,  $\rho = 1000$  m,  $\epsilon_r = 5.5$ , and  $\sigma_0 = 0.03$  S/m). (a) Geometry. (b) GO field at the tunnel entrance ( $s = 0$  m). (c) PE field at  $s = 100$  m. (d) PE field at  $s = 200$  m. (e) PE field at  $s = 300$  m.

$t_0(q)$  can be used to give a practical estimate of the mode attenuation per unit length  $\alpha_z$  [dB/km] =  $-8686 \operatorname{Re} P_{22}$

$$\alpha_z^{mn} [\text{dB/km}] \approx 4343 \lambda^2 \operatorname{Re} \left( \frac{1}{Z_\perp} \right) \frac{n^2}{b^3} + 4343 \lambda^2 \operatorname{Re} Z_\parallel \cdot \begin{cases} \frac{2}{\lambda^2 \rho}, & t_0^+ \gg 1 \\ \left[ \frac{m^2}{(2a)^3} + \frac{8(2a)^3(15 - m^2 \pi^2)}{3\pi^2(m\lambda)^4 \rho^2} \right], & t_0^+ \ll -1 \end{cases} \quad (29)$$

(effects of torsion are neglected). A similar formula holds for the horizontally polarized modes if  $Z_\parallel$ ,  $Z_\perp$  are replaced with the corresponding admittances  $Y = 1/Z$ . The accuracy of the practical formulae can be inferred from Fig. 3, where the solid

lines depict the attenuation of the two lowest order modes of the curved rectangular waveguide considered in [7], and the crosses represent the asymptotic estimates (29) for the two respective limits. A comparison with Mahmoud and Wait's numerical results taken from [7, fig. 3] (white and black circles) shows a good agreement for moderate values of the relative tunnel curvature  $a/\rho$ .

In the validity region of (22) [first line of (29)], the main part of the whispering gallery mode attenuation is caused by ohmic and refraction losses in the concave side wall  $y = -a$  and rapidly tends, with increasing tunnel height and carrier frequency, to its limit  $8686 \operatorname{Re} Z_\parallel / \rho$  depending only on the tunnel axis curvature and wall impedance. In the opposite case of an almost straight tunnel [second line of (29)] this formula gives a small (proportional to the second power of curvature) additional

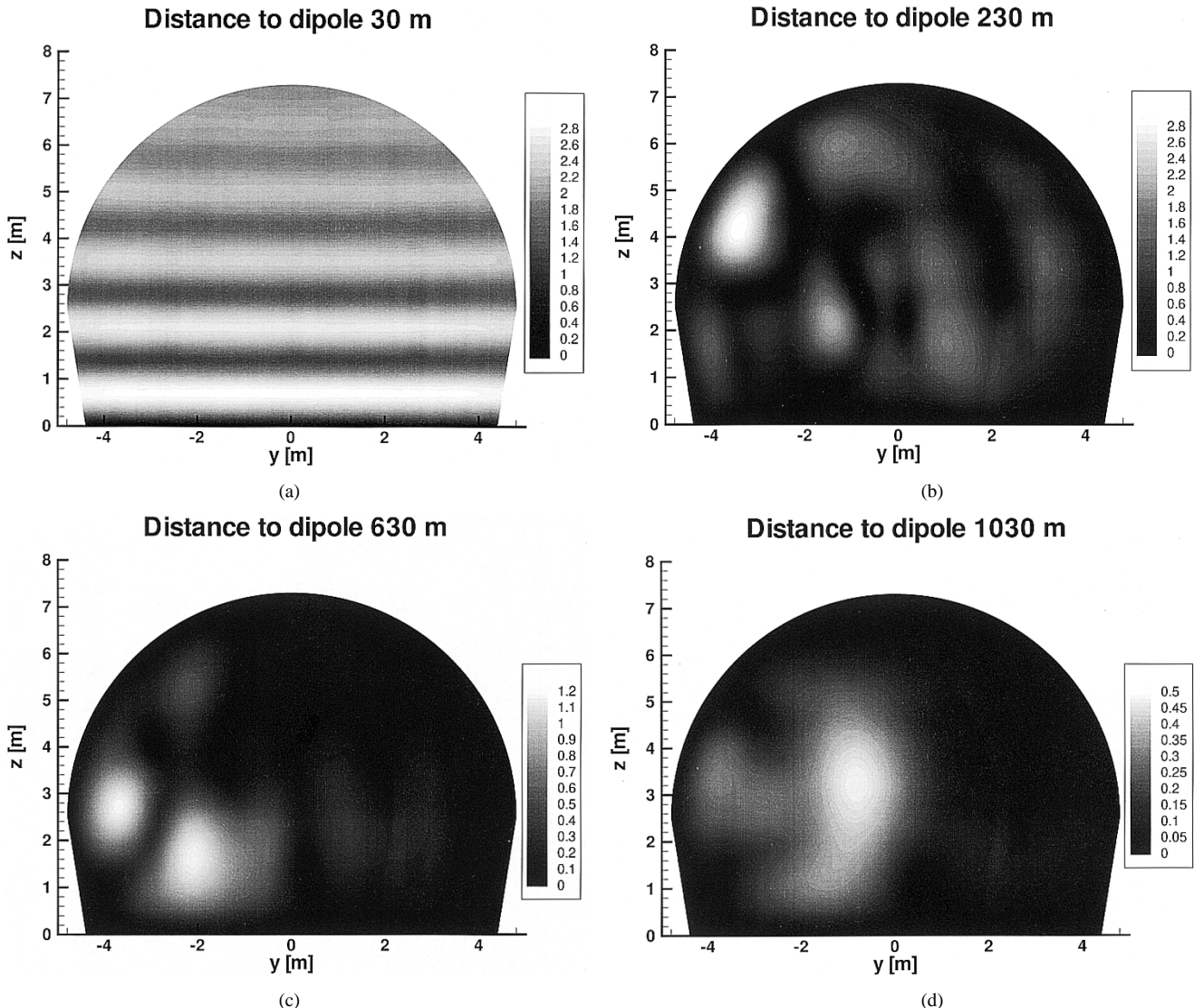


Fig. 5.  $|V(y, z)|$  in an arched tunnel at different distances to a vertical half-wavelength dipole placed 30 m outside the tunnel entrance and 3.6 m above the ground ( $f = 900$  MHz,  $\rho = 800$  m,  $\epsilon_r = 5.5$ , and  $\sigma_0 = 0.03$  S/m). The tunnel cross section consists of a half-circle of radius 4.8 m and a trapezoid of widths 9.6 m and 8.8 m and of height 2.5 m. (a) GO field at the tunnel entrance ( $s = 0$  m). (b) PE field at  $s = 200$  m. (c) PE field at  $s = 600$  m. (d) PE field at  $s = 1000$  m.

frequency- and index-dependent damping, compared with the generally used approximation

$$\alpha_z^{mn}[\text{db/km}] \approx 4343\lambda^2 \left[ \text{Re.} \left( \frac{1}{Z_\perp} \right) \frac{n^2}{b^3} + \text{Re.} Z_{\parallel} \frac{m^2}{(2a)^3} \right] \quad (30)$$

Asymptotic estimate (29), coinciding with the direct numerical solution of the rigorous PE eigenvalue problem (19) to the accuracy of about 1%, agrees with the published results on low-order mode attenuation in rectangular waveguides (cf. [7]–[9]), which validates the proposed approximate solution. Our approach can also simplify testing the approximate practical estimates of the propagation losses in arched tunnels. So, in the case of a circular cross section of diameter  $d$ , inserting Bessel function  $w(r) = J_0(j_0, 12r/d)$  into the integrals (10) gives immediately  $\alpha$  [db/km] =  $5090(Z + Y)\lambda^2/d^3$  which was the starting point for Yamaguchi's "equiareal" formula [9].

A rough *a priori* applicability condition of the PE method follows from expanding the mode propagation wavenumber in powers of its transversal wavenumbers:

$$k_s = \sqrt{k^2 - k_y^2 - k_z^2} = k - \frac{k_y^2 + k_z^2}{2k} - \frac{(k_y^2 + k_z^2)^2}{8k^3} + \dots \quad (31)$$

As is well known (e.g., [15], [26]), the "parabolic" approximation corresponds to the first two terms of this series. Therefore, the phase-error accumulation, limiting the applicability of the PE, has the order of magnitude  $s(k_y^2 + k_z^2)^2/8k^3$ . Estimating the transversal wave numbers by their explicit values for a perfectly lossless rectangular waveguide, one comes to the following PE validity criterion (cf. [26])

$$\delta\Phi \approx \frac{\pi\lambda^3 s}{64} \left[ \left( \frac{m}{2a} \right)^2 + \left( \frac{n}{b} \right)^2 \right]^2 \ll \pi. \quad (32)$$

Taken together with the above estimates of the waveguide mode attenuation (29), it enables one to find the range  $s$  within which PE accurately describes all essentially contributing modes.

## V. MODELING RADIO WAVE PROPAGATION IN TUNNELS

The advantages of the vectorial PE derived in Section III manifest themselves when solving practical problems of radiowave propagation in tunnel environments. Not being able to extensively describe here all possible applications, we confine ourselves with two realistic examples demonstrating its versatility and computational efficiency.

Even in the simplest case of a rectangular tunnel cross section, the straightforward numerical integration of the vectorial PE is usually more efficient than semianalytical solutions based on separation of variables. Apart from the purely computational advantages demonstrated, e.g., in [15], [17], [26], the flexibility and physical adequacy of the PE [13], [14] allows one to easily adapt it to different propagation scenarios. As an example, consider the entrance of a rectangular road tunnel illuminated from outside by a vertical dipole. To predict the field strength inside the tunnel, the diffraction by the edges of the entrance aperture as well as the blockage by passing-by vehicles must be taken into account. In a rigorous formulation, such a diffraction problem can hardly be solved with modest computational means. However, in the framework of physical optics, the Kirchhoff approximation readily yields a simple and sufficiently accurate solution [27]. As PE is equivalent to the paraxial physical optics [14], [26], the aforementioned diffraction effects can be simulated numerically with a minimum modification of the standard computational scheme (for example, the vehicles can be represented as opaque screens of the corresponding shape). The results of such modeling are depicted in Fig. 4 showing cross-sectional field distributions in a rectangular tunnel with a car in the left lane and a truck in the right lane obstructing the dipole radiation coming into the tunnel entrance aperture. Although the Kirchhoff approximation does not describe correctly higher diffraction angles, the resulting discrepancy dies out rapidly with range due to the selective absorption in the tunnel walls (see Introduction and Section II).

Generally, to solve the boundary value problem, namely the vectorial PE (12) subject to BC (13), we use either the Crank–Nicolson FD/FE scheme with a sparse matrix solver or FD splitting methods (e.g., [22]). The efficiency of these techniques for solving realistic problems of radiowave propagation and scattering has been demonstrated in [17], [18]. To cope with the arbitrary tunnel cross section, second order isotropic quadrilateral and triangular elements of Serendipity family have been chosen [28], [29]. These techniques provide a fast and accurate solution of (12) and make thereby the parabolic equation method very powerful in the numerical study of diffraction and propagation of high-frequency electromagnetic waves. The verification of the computer program implementing the vectorial PE has been carried out successfully with the help of the rectangular waveguide eigenfunctions described in the previous section and the numerically obtained eigenfunctions for arched tunnels.

As the parabolic approximation fails near the radiation source [13], it must be replaced there with another solution. In order to obtain the initial values for PE integration, we use the GO part of a computer program written for predicting wave propagation in complex environments [23]. This program calculates the elec-

tric field produced by the source and an appropriate number of its reflections from the earth surface or tunnel walls. This combination enables one to study numerically the complete propagation range of interest, a task which can be performed neither by GO nor by modal analysis. An example of field calculations in an arched tunnel is given in Fig. 5.

## VI. CONCLUSION

By rearranging the asymptotic solution of the Maxwell equations for lossy oversized nonuniform waveguides [12], a two-component vectorial PE governing TE fields in the tunnel cross section is derived. Two field components are coupled weakly on the tunnel walls via a Leontovich-type matrix impedance condition. After having proved the uniqueness of the solution to this boundary value problem, the eigenfunctions for tunnels with a rectangular cross section have been studied for validation purposes. The approximate mode attenuation constants in such tunnels obtained through asymptotic analysis agree in specific cases with published results. In the general case, the vectorial PE is solved using either a Crank–Nicolson FD/FE scheme with a sparse matrix solver or FD-splitting techniques. Asymptotic analysis demonstrates the influence of the waveguide curvature and wall impedances on radio wave propagation characteristics. Numerical examples show 3-D field distributions in realistic tunnels.

To our knowledge, this method gives a more complete and accurate description of radio wave propagation than other existing approaches. Not only is a deeper understanding of the propagation processes in tunnels gained, but also the realistic design and optimization of radio communication systems in such environments are made possible without excessive computational work.

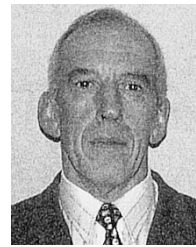
## ACKNOWLEDGMENT

The authors would like to thank Prof. F. M. Landstorfer, Universität Stuttgart, Germany, and V. A. Vinogradov, IZMIRAN, Troitsk, Russia, for their support. They would also like to thank two reviewers for their constructive comments, which helped them to improve this paper essentially.

## REFERENCES

- [1] P. Delogne, “EM propagation in tunnels,” *IEEE Trans. Antennas Propagat.*, vol. 39, pp. 401–406, Mar. 1991.
- [2] S. F. Mahmoud and J. R. Wait, “Geometrical optical approach for electromagnetic wave propagation in rectangular mine tunnels,” *Radio Sci.*, vol. 9, no. 12, pp. 1147–1158, 1974.
- [3] S.-H. Chen and S.-K. Jeng, “SBR image approach for radio wave propagation in tunnels with and without traffic,” *IEEE Trans. Veh. Technol.*, vol. 45, pp. 570–578, Aug. 1996.
- [4] J. S. Lamminmäki and J. J. A. Lempäinen, “Radio propagation characteristics in curved tunnels,” *Inst. Elect. Eng. Proc. Microwave Antennas Propagat.*, vol. 145, pp. 327–331, Aug. 1998.
- [5] Y. Zhang, Y. Hwang, and R. G. Kouyoumjian, “Ray-optical prediction of radio-wave propagation characteristics in tunnel environments—Part 2: Analysis and measurements,” *IEEE Trans. Antennas Propagat.*, vol. 46, pp. 1337–1345, Sept. 1998.
- [6] D. Didascalou, F. Küchen, and W. Wiesbeck, “Ein neuartiges Normierungsverfahren für die strahlenoptische Wellenausbreitungsmodellierung in beliebig geformten Tunneln,” *Frequenz*, vol. 53, no. 9/10, pp. 182–188, 1999.
- [7] S. F. Mahmoud and J. R. Wait, “Guided electromagnetic waves in a curved rectangular mine tunnel,” *Radio Sci.*, vol. 9, no. 5, pp. 567–572, 1974.

- [8] A. G. Emslie, R. L. Lagace, and P. F. Strong, "Theory of the propagation of UHF radio waves in coal mine tunnels," *IEEE Trans. Antennas Propagat.*, vol. AP-23, pp. 192–205, Mar. 1975.
- [9] Y. Yamaguchi, T. Abe, T. Sekiguchi, and J. Chiba, "Attenuation constants of UHF radio waves in arched tunnels," *IEEE Trans. Microwave Theory Tech.*, vol. MTT-33, pp. 714–718, Aug. 1985.
- [10] Y. A. Kravtsov and Y. I. Orlov, *Geometrical Optics of Inhomogeneous Media*. Berlin, Germany: Springer-Verlag, 1990, vol. 6, Springer Ser. Wave Phenomena.
- [11] Lord Rayleigh, "The problem of the whispering gallery," *The London, Edinburgh, Dublin Philosoph. Mag. J. Sci.—Ser. 6*, vol. 20, no. 120, pp. 1001–1004, 1910.
- [12] V. A. Baranov and A. V. Popov, "Adiabatic modes of curved EM waveguides of arbitrary cross section," in *Proc. 13th ACES*, Monterey, CA, Mar. 1997, pp. 1036–1041.
- [13] V. A. Fock, *Electromagnetic Diffraction and Propagation Problems*. Oxford, U.K.: Pergamon, 1965, vol. 1, Int. Ser. Monographs Electromagn. Waves.
- [14] G. D. Malyuzhinets, "Developments in our concepts of diffraction phenomena," *Soviet Physics: Uspekhi*, vol. 69(2), no. 5, pp. 749–758, 1959.
- [15] F. D. Tappert, "The parabolic approximation method," in *Wave Propagation and Underwater Acoustics*, J. B. Keller and J. S. Papadakis, Eds. New York: Springer-Verlag, 1977, ch. 5.
- [16] V. M. Babić and V. S. Buldyrev, *Short-Wavelength Diffraction Theory: Asymptotic Methods*. Berlin, Germany: Springer-Verlag, 1991, vol. 4, Springer Ser. Wave Phenomena.
- [17] A. A. Zaporozhets and M. F. Levy, "Radar cross-section calculation with marching methods," *Electron. Lett.*, vol. 34, no. 20, pp. 1971–1972, 1998.
- [18] A. A. Zaporozhets, "Application of vector parabolic equation method to urban radiowave propagation problems," *Inst. Elect. Eng. Proc. Microwave Antennas Propagat.*, vol. 146, no. 4, pp. 253–256, 1999.
- [19] A. V. Popov, V. A. Vinogradov, N. Y. Zhu, and F. M. Landstorfer, "3-D parabolic equation model of EM wave propagation in tunnels," *Electron. Lett.*, vol. 35, no. 11, pp. 880–882, 1999.
- [20] R. S. Meyerova, A. V. Popov, and S. A. Hoziosky, "Low order modes transformation in smooth waveguide couplings," *Radio Sci.*, vol. 22, no. 6, pp. 1009–1012, 1987.
- [21] T. B. A. Senior and J. L. Volakis, *Approximate Boundary Conditions in Electromagnetics*. London, U.K.: Inst. Elect. Eng., 1995, vol. 41, IEE Electromagn. Wave Ser.
- [22] C. A. J. Fletcher, *Computational Techniques for Fluid Dynamics. Volume I: Fundamental and General Techniques*, ser. Springer Ser. Computat. Phys.. New York: Springer-Verlag, 1997.
- [23] N. Y. Zhu, F. M. Landstorfer, and G. Greving, "Three-dimensional terrain effects on high frequency electromagnetic wave propagation," in *Proc. Eur. Microwave Conf.*, Stuttgart, Germany, Sept. 1991, pp. 1205–1210.
- [24] A. V. Popov, "Numerical solution of the wedge diffraction problem by the transverse diffusion method," *Soviet Phys.: Acoust.*, vol. 15, no. 2, pp. 226–233, 1969.
- [25] *Handbook of Mathematical Functions*, M. Abramowitz and I. A. Stegun, Eds., Dover, New York, 1972.
- [26] Y. V. Kopylov, A. V. Popov, and A. V. Vinogradov, "Application of the parabolic wave equation to X-ray diffraction optics," *Opt. Commun.*, vol. 118, pp. 619–636, 1995.
- [27] M. Born and E. Wolf, *Principles of Optics*, 6 (corrected) ed. Cambridge, U.K.: Cambridge Univ. Press, 1997.
- [28] O. C. Zienkiewicz, *The Finite Element Method*, 3 ed. London, U.K.: McGraw-Hill, 1977.
- [29] N. Y. Zhu and F. M. Landstorfer, "An efficient FEM formulation for rotationally symmetric coaxial waveguides," *IEEE Trans. Microwave Theory Tech.*, vol. 43, pp. 410–415, Feb. 1995.



**Alexei V. Popov** (M'93) was born in Krasnoyarsk, Russia, in 1940. He received the M.Sc. degree from Moscow Institute of Physics and Technology (MFTI) in 1964 and the Ph.D. and Dr.Sci. (mathematics and physics) degrees from the Acoustics Institute, Moscow, in 1969 and 1986, respectively.

From 1969 to 1973, he worked at the Computing Center of Latvian State University, Riga. He joined the Institute of Terrestrial Magnetism, Ionosphere, and Radiowave Propagation, Troitsk, Moscow, Russia, in 1973. Since 1996, he has been with the Moscow X-ray Optics Group, Lebedev Physics Institute. His main interests include diffraction theory, asymptotic methods (perturbation theory, parabolic wave equation), radiowave propagation, ground penetrating radar, and X-ray optics.

Dr. Popov is a member of the International Informatization Academy. He was awarded the U.S.S.R. State Prize in engineering in 1990.



**Ning Yan Zhu** (S'89–M'91) was born in Nanjing, China, in 1960. He received the B.Sc. degree from the East China Engineering Institute, Nanjing, China, in 1982, and the Dipl.-Ing. and Dr.-Ing. degrees from the Technische Universität München and the Universität Stuttgart, Germany, in 1986 and 1990, respectively.

He is currently a Staff Member of the Institut für Hochfrequenztechnik, Universität Stuttgart, Germany. His main interest is in using analytic and numerical methods to solve diffraction and scattering problems.